A TEST RESULT ON POSITIONAL ACCURACY OF KOMPSAT-2 PAN IMAGERY

Jaehong Oh, PhD candidate
Satellite Positioning and Inertial Navigation (SPIN) Laboratory,
The Ohio State University
470 Hitchcock Hall, 2070 Neil Ave, Columbus, OH 43212
oh.174@osu.edu

Changno Lee, Associate Professor
Seoul National University of Technology,
172 Gongreung 2-dong, Nowon-gu, Seoul 139-743, Korea
changno@snut.ac.kr

Doo Chun Seo, Senior Researcher
Korea Aerospace Research Institute,
115 Gwahangno, Yuseong-Gu, Daejeon, Korea
dcivil@kari.re.kr

ABSTRACT

KOMPSAT-2 (KOrea Multi-Purpose SATellite-2) was launched in July 28 2006 with specification of one-meter resolution panchromatic and four-meters resolution multi spectral sensors in 15km swath width. To help understand KOMPSAT-2 positional accuracy, this paper reports a test result on accuracy of three KOMPSAT-2 images covering the same area. For the purpose, a number of ground points were acquired from the bundle adjusted stereo aerial images over the entire target area. First, accuracy of the provided RPC and ephemeris data was tested and analyzed. Second, indirect georegistration was attempted to improve the accuracy by modeling geometric errors based on RPC correction and physical sensor modeling. For RPC correction, shift-only, affine, and second order polynomial models were tested. The physical sensor modeling was carried out by estimating constant bias or linear drift in the attitude angles. In the last, ground restitution accuracy was analyzed even though the across track image pairs do not have optimal convergence angle for restitution.

KEYWORDS: KOMPSAT-2, Accuracy, RPC, Physical model, Ephemeris

INTRODUCTION

High-resolution satellite imagery has become very useful geospatial information not only for military purpose, e.g. reconnaissance, but also for civilian applications, e.g. base image map. Recognizing importance of geospatial imagery, many countries have made efforts to secure independent operation of high performance satellites (Stoney, 2008). Keeping pace with the development of the satellites, the Korea Multi-Purpose Satellite-2 (KOMPSAT-2) was launched in 28 July 2006 at Plesetsk Cosmodrome in Northern Russia to collect one-meter panchromatic and four-meter multi-spectral images with a 15 km swath width from a pushbroom sensor-based multi-spectral camera (MSC) (Seo et al., 2008).

To make the geospatial image more useful, one of the most important preprocessing is to achieve high positional accuracy on the ground. KOMPSAT-2 level 1R data includes ephemeris data providing the epoch, satellite's position, velocity, and attitude angles as well as Rational Polynomial Coefficients (RPCs). Therefore, users can select and use either the physical sensor model or Rational Function Model (RFM) (OGC, 1999). Without any ground control, the horizontal positional accuracy of monoscopic KOMPSAT-2 imagery is known about 80 meters at 90% circular significance after processing precise orbit and attitude determination (Seo et al., 2008).

There are not many research conducted on positional accuracy of KOMPSAT-2. Seo et al. (2008) tested KOMPSAT-2 level 1G PAN for worldwide area using ground controls extracted from IKONOS ortho-rectified images by Google Earth. The authors reported horizontal accuracy of 51.65 meters at 90% significance when physical sensor modeling is used. Saunier et al. (2008) presented a level 1R data accuracy which is 40 meters of horizontal RMSE without any ground control, and 6.6 meters of RMSE when single ground control is used to make shift correction to

RPC. Nowak Da Costa and Walczynska (2010) presented the geometric quality results of four orthorectified KOMPSAT-2 level 1R images using various ground control distributions. RPC and the rigorous model in PCI Geomatics and ERDAS LPS are used for orthorectification, and 2.1m and 4m of RMSE were reported for Easting and Northing respectively. The authors concluded that the accuracy is sensitive to the off-nadir angle and ground control distribution, not to the number of controls. In addition, it was shown that the affine-based RPC correction could yield similar result to Toutin's rigorous model.

This study carried out positional accuracy analysis, not only using RPC, also using provided ephemeris data of three KOMPSAT-2 level 1R images covering the same area. Ground controls over the entire region were extracted from bundle adjusted aerial images. First, positional accuracy of the provided RPC and ephemeris data is assessed, followed by adjustment of the RPC and the ephemeris information, aided by ground controls. Several cases of parameterization were tested for the adjustment, and geometric error pattern was analyzed considering the point location in the image, not just providing total RMSE. Finally, ground restitution accuracy was tested even though the across track image pairs do not have optimal convergence angle.

This paper is structured as follows: first, two methods for KOMPSAT-2 georegistration will be briefly explained in the next section; second, experimental results are presented; the summary and conclusion follow in the end.

KOMPSAT-2 IMAGE GEOREGISTRATION

KOMPSAT-2 level 1R data includes both ephemeris data and RPC to enable image georegistration based on either physical sensor modeling or replacement sensor modeling. Below is presented a brief explanation about the two models.

Physical Sensor Modeling using Ephemeris Data

KOMPSAT-2 MSC is basically modeled using the collinearity equation such as the generic pushbroom model, expressed as Eq. (1). The model is in non-linear form for computing a coordinate in the sensor frame, (x, y, z), from a given ground coordinate in the Earth Centered Earth Fixed (ECEF) frame, (X, Y, Z). Other terms can be computed using the provided KOMPSAT-2 ephemeris data which contains the epoch, satellite's position, velocity, and attitude angles for direct georegistration. Given an instant time, the exterior orientation parameters (EOPs) can be computed by interpolation (KARI, 2008).

$$\begin{bmatrix} x \\ y \\ z \end{bmatrix} = k \underbrace{M_{Body}^{Sensor} M_{Orbit}^{Body} M_{ECEF}^{Orbit}}_{=M} \begin{bmatrix} X - X_L \\ Y - Y_L \\ Z - Z_L \end{bmatrix} \quad (1)$$

Where, x, y, z is the coordinate in the sensor frame (y is the flight direction, z is direction to the surface of the earth, and x completes the right handed system), $[X \quad Y \quad Z]^T$ is the ground point coordinate in the ECEF frame, $\vec{P} = [X_L \quad Y_L \quad Z_L]^T$ is the satellite position in the ECEF frame, M_{ECEF}^{Orbit} is the time-dependent rotation matrix from the ECEF frame to the orbit frame, M_{Orbit}^{Body} is the time-dependent rotation matrix from the orbit coordinate frame to the body frame, M_{Body}^{Sensor} is the rotation matrix from the body frame to the sensor frame, and k is the scale factor.

From the provided ephemeris data, rotation matrices can be computed using Eqs.(2)-(5). First, the rotation matrix from the ECEF frame to the orbit frame, M_{ECEF}^{Orbit}, is obtained by the direction cosine, which is computed from the position and velocity vector in the ephemeris. Note that the X direction in the velocity vector is along the flight direction, the Y direction is perpendicular to the orbit plane, and the Z direction is down to the earth's center.

$$M_{ECEF}^{Orbit} = \begin{bmatrix} \vec{X}^T \\ \vec{Y}^T \\ \vec{Z}^T \end{bmatrix} \tag{2}$$

Where,

$$\vec{Z} = -\frac{\vec{P}}{\left\|\vec{P}\right\|},\ \vec{Y} = \frac{\vec{Z}\times\vec{V}}{\left\|\vec{Z}\times\vec{V}\right\|},\ \vec{X} = \vec{Y}\times\vec{Z} \tag{3}$$

The rotation matrix from the orbit coordinate frame to the body frame, M_{Orbit}^{Body}, is computed as Eq.(4) by multiplying consecutive rotation matrices from the attitude angles in the ephemeris data.

$$M_{Orbit}^{Body} = \left(M_{yaw}\cdot M_{pitch}\cdot M_{roll}\right)^T \tag{4}$$

The rotation matrix from the body frame to the sensor frame, M_{Body}^{Sensor}, is used to convert the axis directions as provided Eq.(5).

$$M_{Body}^{Sensor} = \begin{bmatrix} 0 & -1 & 0 \\ -1 & 0 & 0 \\ 0 & 0 & -1 \end{bmatrix} \tag{5}$$

An image coordinates which starts from (0,0) at the upper-left, $(sample, line)$ can be transformed into a coordinate in the sensor frame, (x, y, z), using Eqs.(6) and (7). Note that only sample coordinate is used for the transformation because KOMPSAT-2 MSC is a pushbroom sensor. KOMPSAT-2's interior orientation parameters can be found in the general information data file such as the focal length, f, the CCD pixel size, ρ, and CCD alignment information, (f_x, f_y, l_x, l_y). The example of parameter values are presented in Table 1.

$$\begin{aligned} x &= sample\times\rho + f_x \\ y &= a\times x + b \\ z &= -f \end{aligned} \tag{6}$$

Where,

$$\begin{aligned} a &= \left(l_y - f_y\right)/\left(l_x - f_x\right) \\ b &= f_y - a\times f_x \end{aligned} \tag{7}$$

Table 1. KOMPSAT-2 interior orientation parameters for physical sensor modeling.

Parameter	Value
Focal length	9.022 meters
Pixel Size	13 microns
CCD alignment information for PAN	f_x = -0.0988400, f_y = -0.0906279, l_x = 0.0961600, l_y = -0.0890177

The positional accuracy based on the provided ephemeris data is usually not enough to be used as a base map and for topographic mapping. Therefore, the accuracy should be improved using ground control information. With ground controls, indirect georegistration can be performed which estimate the bias and drift in the position and

attitude information in the ephemeris. Since the trajectory of a spaceborne is smooth and there is high correlation between position and attitude angles, the correction can be made by estimating the bias and drift in attitudes angles as Eq.(8) (Kratky, 1989). Therefore, the collinearity equation, Eq.(1), is linearized with respect to the correction terms, $d\omega_0$, $d\omega_1$, $d\phi_0$, $d\phi_1$, $d\kappa_0$, and $d\kappa_1$, to form the Gauss Markov model and the model is solved by the least square.

$$\begin{aligned} \omega &= \omega^{eph} + d\omega_0 + d\omega_1 \cdot L \\ \phi &= \phi^{eph} + d\phi_0 + d\phi_1 \cdot L \\ \kappa &= \kappa^{eph} + d\kappa_0 + d\kappa_1 \cdot L \end{aligned} \tag{8}$$

Where, ω, ϕ, κ are roll, pitch, yaw angle respectively, the superscript '*eph*' denotes the ephemeris data, and L is the image line number.

Replacement Sensor Model

The Rational Function Model (RFM) is the most popular replacement sensor model which is also in non-linear form with 80 unknowns (or 78 unknowns) to compute an image coordinate, $(sample, line)$, from a given ground coordinate, (φ, λ, h)(latitude, longitude, and height, respectively) (OGC, 1999). The reason of its popularity is because no information about camera and ephemeris is required to perform sensor georegistration while there is little difference in projection accuracy between the RFM and the rigorous model for a given elevation range (Grodecki, 2001).

KOMPSAT-2 also provides RPCs which is nothing but coefficients of RFM. Same with physical sensor modeling, the positional accuracy of RPC can be improved when ground control information is available. But, contrast to physical sensor modeling, RPC based georegistration is rather simple. It is because the correction can be made on a two-dimensional image domain (Dial and Grodecki, 2002; Fraser and Hanley, 2005). Eq. (9) is the second order polynomial model while the affine model is with $a_4 \sim a_6, b_4 \sim b_6$ set zero and shift-only correction model is with only a_1, b_1.

$$\begin{aligned} s' &= a_1 + a_2 \times s + a_3 \times l + a_4 \times s^2 + a_5 \times l \times s + a_6 \times l^2 = \frac{Num_s(U,V,W)}{Den_s(U,V,W)} \\ l' &= b_1 + b_2 \times s + b_3 \times l + b_4 \times s^2 + b_5 \times l \times s + b_6 \times l^2 = \frac{Num_L(U,V,W)}{Den_L(U,V,W)} \end{aligned} \tag{9}$$

where, s, l is the computed image coordinates (sample, line) using the provided RPC and s', l' is the corrected image coordinates (the upper left image coordinate is (0,0)), a, b are correction parameters, Num, Den are third order polynomial functions of normalized object space coordinates, U, V, W.

EXPERIMENT

Data Specification

Three Kompsat-2 (KARI) images covering the same area were tested for the accuracy assessment. Table 2 shows the specification of each tested image. KOMPSAT-2 data has 15,000 sample pixels per each line, and about one meter ground sample distance (GSD). The tested target area is Daegu, Korea which location is about 35.89°N and 128.49°E, and the terrain elevation range is about 400 meters. From stereo aerial images, total 39 ground control points and 38 check points were acquired over the entire area for accuracy check purpose. Figure 1 depicts the distribution of ground points over the data set.

Table 2. Test KOMPSAT-2 data specification.

Data	Level	Site	Date	Incidence/Azimuth	Image size	Spectral
K1	1R	Daegu, Korea	2009-01-03	6.2°/249.1°	15,500 × 15,000	PAN
K2	1R	Daegu, Korea	2009-12-31	14.1°/256.1°	15,500 × 15,000	PAN
K3	1R	Daegu, Korea	2010-02-07	5.8°/91.7°	15,500 × 15,000	PAN

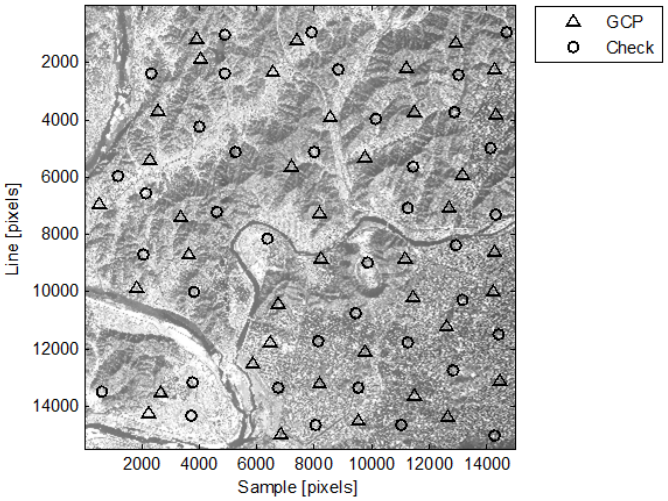

Figure 1. Ground control points and check points distribution on K1 image.

RPC and Ephemeris Data Accuracy

First, the image coordinate error of the provided RPC and ephemeris data was computed by projecting all available ground check points to the images, and the results are presented in Table 3. K1 image has approximately from 30 to 45 pixels of error while K2 and K3 showed rather worse accuracy up to 162 pixels. In K2 and K3, line direction accuracy was far worse than that of column direction. RPC and the ephemeris data showed different results up to a few pixels, mostly in the line direction. This result is not expected because the ephemeris data is supposed to show similar or better accuracy than RPC. Figure 2 depicts the discrepancy between the cases of the ephemeris data and RPC for K1 image along the image line direction. The figure shows linear pattern of discrepancy. Note that the last image line of KOMPSAT-2 level 1R is the first scanned line because KOMPSAT-2 scans from the South to the North. The discrepancy gradually increases with scanning time, which implies that the most probable reason of the discrepancy is due to inaccurate scan rate or scan rate variation. In the implementation, the scan rate was computed based on the first scan line time and the last scan line time. The provided scan rate in the ephemeris file also caused similar discrepancy pattern. Therefore, the provided scan rate may require some corrections. In addition to the scan rate, registration between the panchromatic and multispectral band may affect the discrepancy. Note that KOMPSAT-2's panchromatic sensor's ephemeris data is adjusted referring to the MS1 sensor for 0.5 pixels level of MS1 (corresponding to 2 pixels of the panchromatic sensor), this might have contributed to the discrepancy. More investigations will be required to find out the reason causing this difference.

Table 3. Positional accuracy of the provided RPC and ephemeris data.

		RMSE [pixel]		Max [pixel]	
		Sample	Line	Sample	Line
K1	RPC	42.36	30.46	44.95	40.69
	Ephemeris	42.43	34.97	45.12	44.71
K2	RPC	65.66	134.45	67.99	142.55
	Ephemeris	65.72	140.17	68.20	148.38
K3	RPC	30.36	145.57	32.69	156.28
	Ephemeris	30.71	151.92	33.09	162.13

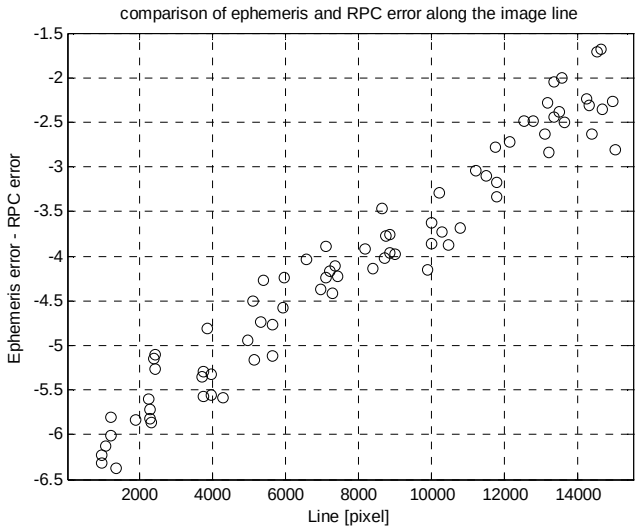

Figure 2. Discrepancy between ephemeris error and RPC error along the line direction (K1 image).

Accuracy of RPC Correction

Table 4 presents the positional accuracy of corrected RPC for the check points. Three correction models were tested; shift, affine, and second order polynomial. Note that the shift correction is to estimate only a_1 and b_1 in Eq.(9). In the table, the shift correction still has large line direction error. Check points errors for K1 and K2 are depicted in Figure 3 where the errors have a kind of rotational pattern. A probable reason would be low heading accuracy, or it may require more accurate boresight calibration. When the affine model is applied, the line direction error could be significantly reduced and one-pixel level of RMSE could be achieved. Figure 4(a) shows the image coordinate errors for K1, K2, and K3 along the sample (column) direction to closely check the error pattern. It can be identified that sample coordinate errors has a 'U' shaped pattern which may indicate requirement of more accurate sensor calibration. Therefore, finally, the second polynomial model was applied, and the error results and pattern were presented in Table 4 and Figure 4(b). No significant error differences were observed compared to the affine model, while the 'U' shaped pattern was slightly mitigated.

Table 4. Positional accuracy of RPC correction.

RPC Correction		RMSE [pixel]		Max [pixel]	
		Sample	Line	Sample	Line
Shift	K1	1.02	5.34	2.72	10.70
	K2	1.16	4.70	2.98	8.26
	K3	1.10	5.58	2.88	10.88
Affine	K1	1.00	1.46	2.50	3.77
	K2	0.99	0.99	2.98	2.26
	K3	0.86	0.87	1.97	2.99
2nd order polynomial	K1	1.12	1.39	2.38	3.88
	K2	1.02	1.01	3.08	2.65
	K3	0.84	0.84	1.72	2.85

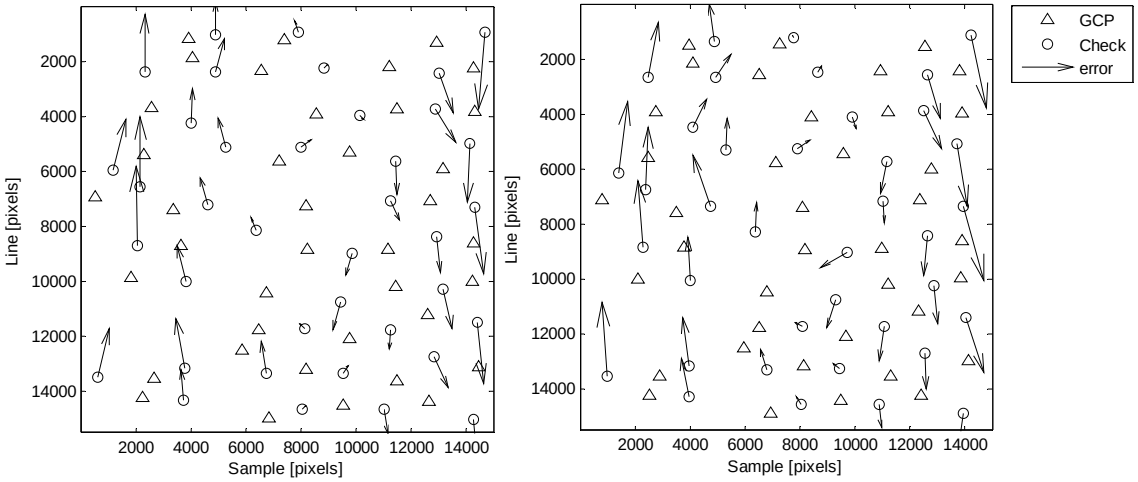

(a) (b)

Figure 3. Error pattern at the check points for RPC shift correction (a) K1, (b) K2

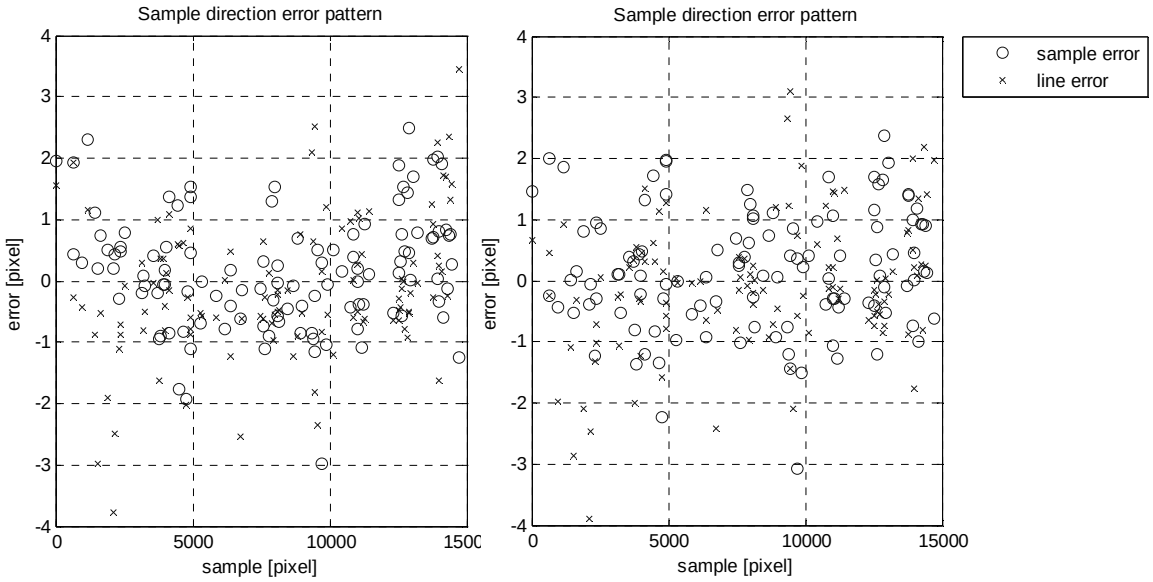

(a) (b)

Figure 4. Error pattern along the sample direction at the check points (errors of K1, K2, and K3 are overlaid), (a) affine based RPC correction, (b) 2nd order polynomial based RPC correction.

Accuracy of Physical Sensor Modeling

Using the same ground controls with the RPC correction test, the physical sensor modeling was carried out based on the provided ephemeris data (exterior orientation information) and general information (interior orientation information). Two cases of exterior orientation parameter models were tested to correct the provided ephemeris data. First, only bias is assumed in the attitude angles and estimated using the ground control. Second, bias and linear drift are estimated in the attitude angles. Table 5 presents the positional accuracy computed for the check points. One pixel level accuracy could be achieved, except K1's line direction. The test result showed that linear attitude correction could improve the line direction accuracy slightly better than the bias-only correction case. The result seems slightly worse than the RPC correction method, but it was not at significant level.

Table 5. Positional accuracy of physical sensor modeling.

Physical modeling		RMSE [pixel]		Max [pixel]	
		Sample	Line	Sample	Line
Constant Attitude correction	K1	1.04	1.73	2.72	3.57
	K2	1.17	1.12	2.96	2.48
	K3	1.08	0.94	2.70	3.09
Linear Attitude correction	K1	1.05	1.41	2.83	3.79
	K2	1.06	0.96	2.87	2.45
	K3	1.04	0.86	2.57	3.16

Ground Restitution Accuracy

Finally, ground restitution accuracy was checked for the check points. Note that the images are not in-track stereo which acquire stereo images in single orbit. In Table 2, it is shown that the image acquisition geometry, i.e. incidence angle and azimuth, does not have good convergence angle for the ground restitution. K2 and K3 pair has approximate 20 degrees of convergence angle. The accuracy test result is presented in Table 6. One-meter level of horizontal and 2~3 meters of vertical RMSE could be obtained. The RPC correction methods showed slightly better ground restitution accuracy.

Table 6. Ground restitution accuracy.

Georegistration Model		RMSE [meters]			Max [meters]		
		X	Y	Z	X	Y	Z
RPC	Affine	0.81	0.98	2.37	2.05	2.74	6.18
	2nd order polynomial	0.79	1.01	2.45	2.02	2.66	5.91
Physical Modeling	Constant Attitude correction	0.98	1.08	3.54	1.93	2.49	8.20
	Linear Attitude correction	0.97	0.90	2.66	2.24	2.65	6.88

CONCLUSION

This study presented a test result on positional accuracy of three KOMPSAT-2 level 1R images covering the same area. Accuracy of both RPC and ephemeris data was tested using the ground check points extracted from bundle adjusted stereo aerial images. Following the direct georegistration accuracy assessment of the provided RPC and ephemeris data, correction was attempted to improve the georegistration accuracy by modeling geometric errors. For RPC correction, shift-only, affine, and second order polynomial models were tested. Ephemeris data correction was made by estimating bias-only in the attitude angles, or estimating bias and linear drift in the attitude angles. In the last, ground restitution accuracy was analyzed, even though the across track image pairs did not have optimal convergence angle for stereo restitution. Test results could be summarized as below.

1. The provided ephemeris data accuracy was lower than RPC data, especially in the line direction which may imply the inaccurate scan rate.
2. Error pattern after applying shift-only RPC correction showed relatively large rotation-like line direction errors, it may be due to inaccurate yaw angle or calibration.
3. Affine based RPC correction could achieve one-pixel level of RMSE while small ‘U’ shaped sample coordinate error pattern was observed along the sample direction.
4. The second order polynomial based RPC correction could slightly mitigate the ‘U’ shaped error pattern, but showed similar RMSE with the affine based method.
5. The physical sensor modeling with linear attitude correction was helpful to reduce the line direction georegistration error, compared to constant attitude correction.
6. The physical sensor modeling showed slightly worse georegistration accuracy than the RPC methods, however it was not at significant level.
7. One meter level of horizontal, and 2-3 meters of vertical RMSE could be achieved by ground restitution, even though the across track stereo images did not have optimal convergence angle.

REFERENCES

Dial, G., and J. Grodecki, 2002, "Block adjustment with rational polynomial camera models," Proceedings of the ACSM-ASPRS 2002 Annual Conference, 22-26 April, Washington DC (American Society for Photogrammetry and Remote Sensing, Bethesda, Maryland), unpaginated CD-ROM.

Fraser, C.S., and H.B. Hanley, 2005, "Bias-compensated RPCs for sensor orientation of high-resolution satellite imagery," Photogrammetric Engineering & Remote Sensing, 71(8):909-915.

Grodecki, J., 2001, "IKONOS stereo feature extraction – RPC approach," Proceedings of ASPRS 2001 Annual Convention, 25–27 April, St. Louis, Missouri (American Society for Photogrammetry and Remote Sensing, Bethesda, Maryland), unpaginated CD-ROM.

KARI, 2008, "KOMPSAT-2 Image data Manual for user," Available: http://earth.esa.int/pub/ESA_DOC/K2_IDM_ver1.1.pdf.

Kratky, V., 1989, "Rigorous photogrammetric processing of SPOT images at CCM Canada," ISPRS Journal of Photogrammetry and Remote Sensing, 44:53-71.

Nowak Da Costa, J.K., and A. Walczynska, 2010, "Geometric Quality Testing of the Kompsat-2 Image Data Acquired over the JRC Maussane Test Site using ERDAS LPS and PCI GEOMATICS remote sensing software", JRC Scientific and Technical Reports.

OGC, 1999, The OpenGIS Abstract Specification. Topic 7: The Earth Imagery Case.

Saunier, S., B. Collet, A. Mambimba, 2008, "New Third Party Mission Quality Assessment. Kompsat-2 Mission", GAEL Consultant. Ref no. GAEL-P232-DOC-005.

Seo, D.C., J. Y. Yang, D. H. Lee, J. H. Song, and H. S. Lim, 2008, "Kompsat-2 Direct Sensor Modeling and Geometric Calibration/Validation," The International Archives of the Photogrammetry, Remote Sensing and Spatial Information Sciences. Vol. XXXVII. Part B1. Beijing.

Stoney, W. E., 2008, "ASPRS Guide to Land Imaging Satellites," Available: http://www.asprs.org/news/satellites/satellites.html.